

Surface Molecular Aggregation Structure of Poly(fluoroalkyl acrylate) Thin Films

Koji Honda¹, Masamichi Morita², Sono Sasaki³, Osami Sakata³, and Atsushi Takahara^{1,4}

¹Graduate School of Engineering, Kyushu University, Hakozaki, Higashi-ku, Fukuoka 812-8581, Japan

²Fundamental Research Department, Chemical Division, Daikin Industries, Ltd., 1-1 Nishi Hitotsuya, Settsu-shi, Osaka 566-8585, Japan

³Japan Synchrotron Radiation Research Institute, Mikazuki, Sayo, Hyogo 679-5198, Japan

⁴Institute for Materials Chemistry and Engineering, Kyushu University, Fukuoka 812-8581, Japan

Fax: 81-92-642-2715, e-mail: takahara@cstf.kyushu-u.ac.jp

Surface molecular aggregation structure of poly(fluoroalkyl acrylate)s [PFA-C_y, where y is the fluoromethylene number of the fluoroalkyl (R_f) group] thin films was characterized by grazing-incidence X-ray diffraction (GIXD). In-plane diffractions corresponding to the hexagonal packing of the R_f groups and out-of-plane diffractions corresponding to the lamellar structures were measured for the PFA-C_y with y ≥ 8 in the surface and bulk regions. This result indicated that the R_f groups were oriented almost perpendicular to the surface and that the lamellar structures of R_f groups were oriented parallel to the surface. Also, a comparison of the GIXD data for original and annealed PFA-C₈ films was carried out. It was revealed that the orientation of R_f groups and regularity of R_f lamellar crystal were improved by annealing treatment. In addition, a comparison of the GIXD profiles between the surface and bulk region was also carried out. It was suggested that the orientation and order of the R_f groups in the surface and bulk region are almost the same

Key words: fluoroalkyl groups, polymer thin film, molecular aggregation structure, GIXD

1. INTRODUCTION

Polymers with fluoroalkyl (R_f) groups show surface characteristics that differ greatly from those of comparable hydrogenated structures: for example, excellent chemical and thermal stability, non-adhesive properties, low friction coefficients, low surface free energies, and non-fouling behavior.^{1,2} Thus, they are highly utilized in industry for the production on various surface treatment chemicals such as water and oil repellents for textiles, surface modifiers for plastic, paper, and metal, and additives for lubricating and antifriction. Most of them are poly(fluoroalkyl acrylate)s with long R_f groups, and these polymers have very lower critical surface tension (γ_c) than the γ_c of polytetrafluoroethylene (PTFE), which is a typical fluoropolymer.³

In the previous report, the authors clarified the water repellent mechanism of poly(fluoroalkyl acrylate) [PFA-C_y, where y is the fluoromethylene number of the R_f groups] thin films.⁴ This water repellent mechanism which seems to reflect the crystalline states at the surface region is important for stable surface properties.^{1,4} However, there is no direct evidence on the surface crystalline states of PFA-C_y thin films.

Grazing incidence X-ray diffraction (GIXD)⁵ enables us to gain direct access to information upon crystalline structure at the film surface by choosing an appropriate condition. Up to date, GIXD has revealed crystalline structure at the film surface of polyimide,^{6,7} poly(pyromellitic dianhydride-oxydiamine),⁸ isotactic polypropylene,⁹ poly(ethylene terephthalate),¹⁰ and high-density polyethylene.¹¹

The authors have studied the surface properties and aggregation structure of fluoroalkyl acrylate polymers with various R_f groups and have attempted to establish guideline for the design of novel high-performance R_f

polymers. In this paper, the authors report the molecular aggregation structure of PFA-C_y thin films evaluated by in-plane and out-of-plane GIXD.

2. EXPERIMENTAL

2.1 Materials

The chemical structure of PFA-C_y is shown in Fig.1. Fluoroalkyl acrylate monomers and 1,1,1,4,4,4-hexafluoro-2,2,3,3-tetrachlorobutane (CFC-316) were provided by Daikin Industries Co., Ltd. PFA-C_y were prepared by radical polymerization under nitrogen atmosphere in 3,3-dichloro-1,1,1,2,2-pentafluoropropane (HCFC-225) at 323 K for 18 hours for y=1, 2, 4, 6, and 8, and in CFC-316 at 363 K for 18 hours for y=10, using azobisisobutyronitrile (AIBN) as an initiator.¹² The polymers, except for PFA-C₁, were purified by precipitation in methanol. PFA-C₁ was precipitated in hexane. PFA-C₁, C₂, C₄, and C₆ were obtained as rubbery solids and PFA-C₈ and C₁₀ were obtained as a white powder.

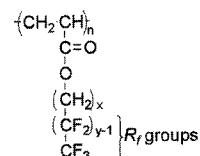


Fig.1 Chemical structure of poly(fluoroalkyl acrylate)s [PFA-C_y, where y is the fluoromethylene number of the R_f group] (x=1 for y=1 and 2, x=2 for y=4, 6, 8, and 10)

PFA-C_y, except for PFA-C₁₀, was dissolved in HCFC-225 (concentration; 1 wt%), and Si-wafer was coated with solution by the spin-coating method (2000 rpm, 30 s). PFA-C₁₀ was dissolved in CFC-316 (concentration; 2 wt%) by heating at 373 K, and the

Si-wafer was coated with the solution at 373 K by the same method, as this polymer could not be dissolved in HCFC-225 and CFC-316 at room temperature. The film thickness was estimated as approximately 100 nm by atomic force microscope measurement (AFM). The AFM observation was performed with an SPA 4000 (Seiko Instruments Inc.). AFM images were obtained under constant force mode in air at 300 K using a 100 μm x 100 μm scanner and a Si_3N_4 tip on a triangle cantilever with a spring constant of 0.032 Nm^{-1} . The films were not annealed, unless it is mentioned otherwise.

2.2 Measurement

GIXD measurements were carried out for the films at 300 K with a six-axis diffractometer installed at a BL-13XU beamline of SPring-8 (Japan Synchrotron Radiation Research Institute, Hyogo, Japan). The wavelength, λ , of monochromatized incident X-rays used in this study was 0.1284 nm (in-plane) or 0.1025 nm (out-of-plane). The data collection time was 1.5 s per step, and the angular interval between steps was 0.05°. Fig.2 shows the schematic geometry of the in-plane and out-of-plane GIXD measurement. When the incident angle, α_i , is equal to, or smaller than, the critical angle, α_c , the incident X-rays undergo total external reflection and penetrate into the samples as evanescent waves. The penetration depth (d_p) of evanescent waves is defined as a depth, at which the intensity decrease to be e^{-1} , and is expressed by

$$d_p = \frac{1}{\sqrt{2k \left\{ \sqrt{(\alpha_c^2 - \alpha_i^2)^2 + 4\beta^2} + \alpha_c^2 - \alpha_i^2 \right\}^{1/2}}} \quad (1)$$

where k is wave vector and β is defined as $\mu\lambda/4\pi$, and μ is linear absorption coefficient. And, the α_c value is given by

$$\alpha_c = \left(\frac{\lambda^2 r_e N}{\pi} \right)^{1/2} \quad (2)$$

where r_e is classical electron radius and N is electron density per unit volume of materials. For our experimental condition with $\lambda = 0.128$ nm or 0.103 nm, the α_c is calculated to be 0.125° or 0.100°, respectively. Thus, Bragg diffraction was obtained from surface and bulk regions at $\alpha_i = 0.10^\circ$ or 0.08° and 0.20° or 0.16° respectively.¹³ In the in-plane geometry, scattering vector (q_{xy}) is parallel to the surface, and the detected profiles reflect information upon crystalline structure perpendicular to the film surface. On the other hand, information about the structure parallel to the surface is obtained from out-of-plane geometry. In this case, a peak position obtained experimentally should be corrected because it was slightly shifted from the corresponding Bragg angle due to reflection of incident X-rays at the sample surface. The value of this shift ($\Delta 2\theta$) is expressed by¹⁴

$$\Delta 2\theta = \alpha_i - \frac{1}{\sqrt{2}} \left\{ \left[(\alpha_i^2 - \alpha_c^2)^2 + 4\beta^2 \right]^{1/2} - \alpha_i^2 + \alpha_c^2 \right\}^{1/2} \quad (3)$$

From this equation, the $\Delta 2\theta$ values for $\alpha_i = 0.08^\circ$ and 0.16° were 0.080° and 0.039° , respectively.

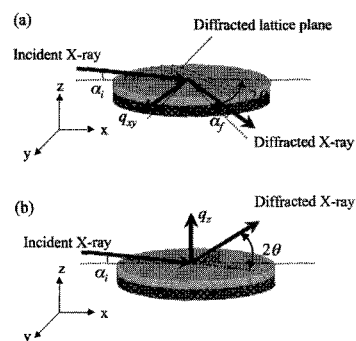


Fig.2 Schematic geometry of (a) in-plane and (b) out-of-plane GIXD measurements.

3. RESULT AND DISCUSSION

3.1 GIXD measurement

Fig. 3 and 4 show the in-plane and out-of-plane GIXD profiles of surface and bulk region measured for PFA-C_y thin films ($y = 1, 2, 4, 6, 8$, and 10 for in-plane GIXD, $y = 8$ and 10 for out-of-plane GIXD). The scattering vector (q) was defined as $(4\pi/\lambda)\sin\theta$. In the case of in-plane GIXD profiles (Fig.3), each PFA-C_y with $y \leq 6$ had a broad and weak peak around $q_{xy} = \text{ca. } 12.5 \text{ nm}^{-1}$ in the profiles. On the other hand, sharp and strong peaks were observed for each PFA-C_y with $y \geq 8$ at $q_{xy} = \text{ca. } 12.5 \text{ nm}^{-1}$. The d -spacing calculated from the peak position was ca. 0.50 nm, that was close to the intermolecular distance between helical chains of PTFE hexagonal ($d = 0.49 \text{ nm}$) phase.¹⁵⁻¹⁷ Therefore, it was suggested that the rigid rod-like R_f groups formed hexagonal packing in the films of PFA-C_y with $y \geq 8$, and the d -spacing of PFA-C_y with $y \geq 8$ (0.50 nm) was larger than that of PTFE (0.49 nm), indicating that slightly tilted R_f groups might be oriented almost perpendicular to the film surface. In out-of-plane GIXD profiles (Fig. 4), diffraction peaks at $q_z = 1-9 \text{ nm}^{-1}$ were measured. These peaks were assignable to the lamellar structure in which R_f groups are ordered like multilayer (the spacing $d = 3.2 \text{ nm}$ [PFA-C₈] and 3.6 nm [PFA-C₁₀], with these values being in good agreement with the length of the two R_f groups),¹⁸ indicating that the lamellar structure is oriented parallel to the film surface. It was revealed that highly oriented and hexagonally packed fluoroalkyl chains at the surface of PFA-C_y with $y \geq 8$ contributed to the high water repellency of their films.

3.2 Effect of annealing treatment

In-plane and out-plane GIXD profiles for PFA-C₈ were also compared with annealed one at 333 K and 348 K for 6 h. In the case of in-plane GIXD, before annealing, sharp and strong diffractions were observed for PFA-C₈ at peak position of $q_{xy} = 12.4 \text{ nm}^{-1}$ and 3.9 nm^{-1} . A peak at $q_{xy} = 3.9 \text{ nm}^{-1}$ was explained as a diffraction from the lamellar structure. This peak became weak in intensity for PFA-C₈ annealed at 333 K (PFA-C₈*) and disappeared for one annealed at 348 K (PFA-C₈**). Another peak corresponding to the hexagonal packing of the R_f groups became sharper with an increase in annealing temperature. By annealing treatment, some R_f

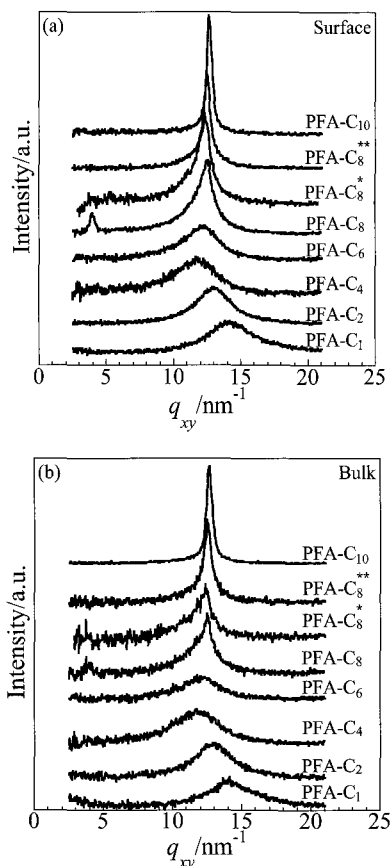


Fig.3 In-plane GIXD profiles measured at (a) surface and (b) bulk region for PFA-C_y thin films (* and ** indicated samples annealed at 333 K and 348 K for 6 h, respectively). The λ of incident X-ray was 0.128 nm.

groups changed their orientation from the parallel direction to the perpendicular one against the film surface. In the case of out-of-plane GIXD, peaks corresponding to the lamellar structure also became sharper with an increase in annealing temperature. From these profile, distortion of the crystal lattice was estimated on the basis of the paracrystalline theory proposed by Hosemann.¹⁹⁻²¹ In the paracrystalline lattice model, the lattice vectors of adjacent unit cells vary in magnitude and direction due to large displacement of lattice points from their ideal positions, resulting in a loss of the long-range crystallographic order. On the assumption that the coordination statistics distribution function for the paracrystalline lattice model is in the form of a Gaussian distribution, the paracrystalline lattice factor $Z(s)$ of the h th-order reflection is defined as

$$Z(s)=Z(h)=[-\exp(-4\pi^2g^2h^2)]/[(1-\exp(-2\pi^2g^2h^2))^2+(4\sin^22\pi h)\exp(-2\pi^2g^2h^2)] \quad (4)$$

Where s is the reciprocal lattice vector, h is the scattering order, and g is the standard deviation of the Gaussian distribution divided by the average lattice vector \bar{a} ; the g is a parameter to evaluate the degree of paracrystalline disorder. The value of g is experimentally given by

$$(\delta\beta)^2 = (1/\bar{a}^2)[(1/N^2) + \pi^4g^4h^4] \quad (5)$$

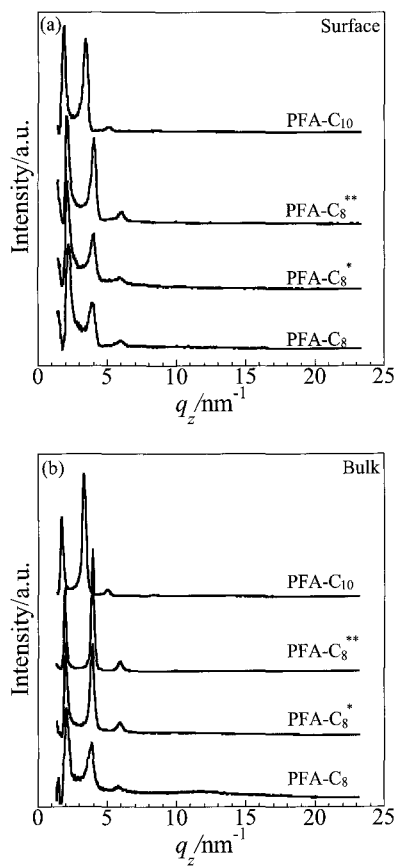


Fig.4 Out-of-plane GIXD profiles measured at (a) surface and (b) bulk region for PFA-C_y with $y \geq 8$ thin films (* and ** indicated samples annealed at 333 K and 348 K for 6 h, respectively). The λ of incident X-ray was 0.103 nm.

Here, $\delta\beta$ is the integral width of a diffraction peak, and N is the number of scattering units. Fig.5 shows a plot of $(\delta\beta)^2$ as a function of h^4 for the (001), (002), and (003) reflections of PFA-C₈ and C₁₀ thin films. A linear relation was obtained between the $(\delta\beta)^2$ and h^4 by the least-squares fitting. The g and N were calculated using eq 5. Fig.6 shows the annealing temperature dependence of g and N for PFA-C₈ and C₁₀ thin films. The g decreased from 5.8×10^{-2} to 4.5×10^{-2} , and N increased from ca. 5 to 9 as increasing annealing temperature. It therefore appears that the paracrystalline distortion was decreased, and that both the orientation and the order of the R_f groups were improved by annealing. PFA-C₁₀ appears to have a sufficiently high order of R_f groups, even without annealing. In the case of PFA-C₁₀, the R_f groups were highly oriented perpendicular to the film surface even for its original films before annealing.

3.3 Comparison between the surface and bulk

In addition, a comparison of the GIXD profiles between the surface and bulk regions was also carried out. The peak positions and half-value width of the diffractions do not show large difference between the surface and bulk regions. It indicates that the orientation and the order of the R_f groups in the surface and bulk region are almost the same. Actually, the paracrystalline distortion was almost the same between the surface and

bulk region (Fig.6).

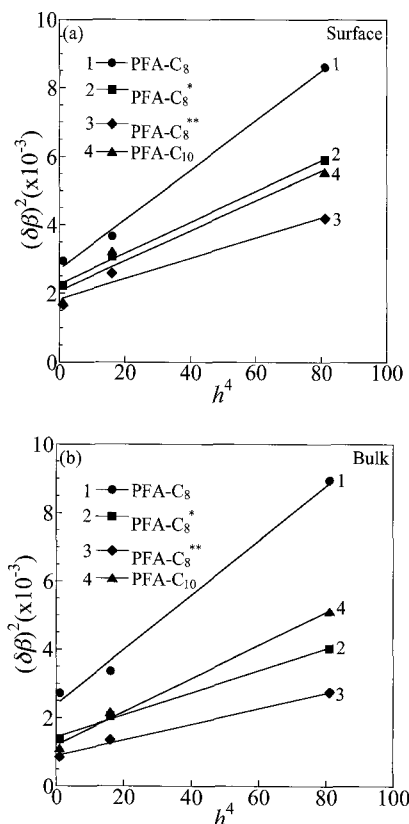


Fig.5 Plot of $(\delta\beta)^2$ as a function of h^4 for the (001), (002), and (003) reflections of PFA-C₈ and PFA-C₁₀ thin films (*annealed at 333 K for 6 h, **annealed at 348 K for 6 h); (a) surface and (b) bulk.

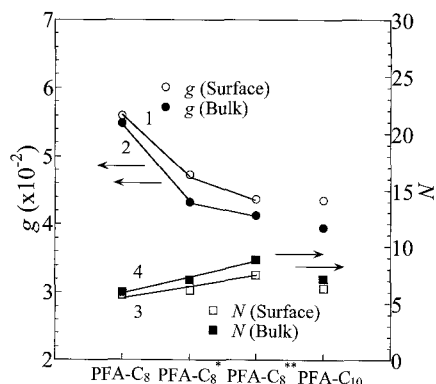


Fig.6 Annealing temperature dependence of g and N for PFA-C₈ and PFA-C₁₀ thin films (*annealed at 333 K for 6 h, **annealed at 348 K for 6 h).

4. CONCLUSION

Molecular aggregation structure of PFA-C_y thin films was evaluated by in-plane and out-of-plane GIXD measurements. In-plane and out-of-plane diffractions for PFA-C_y with $y \geq 8$ suggested the hexagonal packing of R_f groups and the lamellar structure in the thin films. This result indicated that the R_f groups are oriented almost perpendicular and R_f lamellar crystal are parallel to the film surface. It was revealed that highly oriented and hexagonally packed fluoroalkyl chains at the surface of PFA-C_y with $y \geq 8$ led to the high water repellency of

their films. The crystallographic orientation and regularity of the R_f groups were improved by annealing treatment. The orientation and the order of the R_f groups in the surface and bulk region were almost the same.

ACKNOWLEDGEMENTS

This work was partially supported by a Grant-in-Aid for the 21st century COE Program "Functional Innovation of Molecular Informatics" from the Ministry of Education, Culture, Sports, Science, and Technology of Japan. K. H. acknowledges the financial support of Grant-in-Aid for JSPS Fellows. The synchrotron radiation X-ray diffraction experiments were performed at SPring-8 with the approval of Japan Synchrotron Radiation Research Institute (JASRI) as Nanotechnology Support Project of the Ministry of Education, Culture, Sports, Science, and Technology, Japan (Proposal 2003A0606-ND1-np/BL-13XU).

REFERENCES

- [1] A. G. Pittman, "Fluoropolymers", Ed. by L. A. Wall, Wiley-Interscience, New York (1972) pp 419.
- [2] D. L. Schmidt, C. E. Coburn, B. M. Dekoven, G. E. Potter, G. F. Meyers, and D. A. Fischer, *Nature*, **368**, 39 (1994).
- [3] M. K. Bernert and W. A. Zisman, *J. Phys. Chem.*, **66**, 1207 (1962).
- [4] K. Honda, M. Morita, H. Otsuka, and A. Takahara, *Macromolecules*, **38**, 5699 (2005).
- [5] W. C. Marre, P. Eisenberger, and A. Y. Cho, *J. Appl. Phys.*, **50**, 6297 (1979).
- [6] B. J. Factor, T. P. Russell, and M. F. Tony, *Phys. Rev. Lett.*, **66**, 1181 (1991).
- [7] B. J. Factor, T. P. Russell, and M. F. Tony, *Macromolecules*, **26**, 2847 (1993).
- [8] R. F. Saraf, C. Dimitrakopoulos, M. F. Tony, and S. P. Kowalczyk, *Langmuir*, **12**, 2802 (1996).
- [9] N. Kawamoto, H. Mori, K. Nitta, S. Sasaki, and M. Terano, *Angew. Makromol. Chem.*, **256**, 69 (1998).
- [10] M. Durell, J. E. Macdonald, D. Trollev, A. Wehrum, P. C. Jukes, R. A. L. Jones, C. J. Walker, and S. Brown, *Europhys. Lett.*, **58**, 844 (2002).
- [11] H. Yakabe, K. Tanaka, T. Nagamura, S. Sasaki, O. Sakata, A. Takahara, and T. Kajiyama, *Polym. Bull.*, **53**, 213 (2005).
- [12] T. Shimizu, "Modern Fluoropolymers", Ed. by J. Scheris, John Wiley & Sons, New York (1997), pp 507.
- [13] T. P. Russell, *Mater. Sci. Rep.*, **5**, 171 (1990).
- [14] M. F. Tony and S. Brennan, *Phys. Rev. B.*, **39**, 7963 (1989).
- [15] C. W. Bunn and E. R. Howells, *Nature*, **174**, 549 (1954).
- [16] J. M. Corpart, S. Girault, D. Juhué, *Langmuir*, **17**, 7237 (2001).
- [17] Y. Urushihara and T. Nishino, *Langmuir*, **21**, 2614 (2005).
- [18] V. V. Volkov, N. A. Plate, A. Takahara, T. Kajiyama, N. Amaya, and Y. Murata, *Polymer*, **33**, 1316 (1994).
- [19] R. Hosemann, *R. Z. Phys.*, **128**, 1-35 (1950).
- [20] P. H. Lindenmeyer and R. Hosemann, *J. Appl. Phys.*, **34**, 42 (1963).
- [21] R. Hosemann and A. M. Hindeleh, *Macromol. Sci., Phys.*, **B34**, 327 (1995).

(Received December 9, 2006; Accepted February 5, 2007)